Endoplasmic reticulum export and vesicle formation of the movement protein of *Chinese wheat mosaic virus* are regulated by two transmembrane domains and depend on the secretory pathway

Ida Bagus Andika [b,1], Shiling Zheng [a,1], Zilong Tan [c,1], Liying Sun [b,*], Hideki Kondo [d], Xueping Zhou [a], Jianping Chen [b,*]

[a] State Key Laboratory of Rice Biology, Institute of Biotechnology, Zhejiang University, Hangzhou, PR China
[b] State Key Laboratory Breeding Base for Zhejiang Sustainable Pest and Disease Control, Ministry of Agriculture Key Laboratory of Biotechnology in Plant Protection, Institute of Virology and Biotechnology, Zhejiang Academy of Agricultural Sciences, Hangzhou 310021, PR China
[c] College of Chemistry and Life Science, Zhejiang normal University, Jinhua 321004, China
[d] Institute of Plant Science and Resources (IPSR), Okayama University, Kurashiki 710-0046, Japan

ARTICLE INFO

ABSTRACT

The 37K protein of *Chinese wheat mosaic virus* (CWMV) belongs to the 30K superfamily of plant virus movement proteins. CWMV 37K *trans*-complemented the cell-to-cell spread of a movement-defective *Potato virus X*. CWMV 37K fused to enhanced green fluorescent protein localized to plasmodesmata and formed endoplasmic reticulum (ER)-derived vesicular and large aggregate structures. CWMV 37K has two putative N-terminal transmembrane domains (TMDs). Mutations disrupting TMD1 or TMD2 impaired 37K movement function; those mutants were unable to form ER-derived structures but instead accumulated in the ER. Treatment with Brefeldin A or overexpression of the dominant negative mutant of Sar1 retained 37K in the ER, indicating that ER export of 37K is dependent on the secretory pathway. Moreover, CWMV 37K interacted with pectin methylesterases and mutations in TMD1 or TMD2 impaired this interaction in *planta*. The results suggest that the two TMDs regulate the movement function and intracellular transport of 37K.

© 2012 Elsevier Inc. All rights reserved.

Introduction

Plant viruses encode movement proteins (MPs) to facilitate cell-to-cell spread of the viral genome from the initially infected cell(s) through plasmodesmata (PD), the membranous channels that allow intracellular trafficking of molecules between neighboring cells (Maule, 2008; Schoelz et al., 2011). Different types of MP have been recognized and these employ a variety of strategies, but they commonly modify PD to allow the passage of macromolecules such as a viral ribonucleoprotein (vRNP) complex or virions (Benitez-Alfonso et al., 2010). The 30K MP superfamily (Melcher, 2000) is defined by sequence and structural similarities that can be identified among the single MPs encoded by a large number of plant viruses from diverse genera. The 30K *Tobacco mosaic virus* (TMV, genus *Tobamovirus*) MP is the most intensively

studied member of this group and its characteristics and activities are well understood (Heinlein, 2002).

Viral MPs of the 30K superfamily, as well as those of the triple gene block (TGB) family, double gene block family and the small closterovirus MP, associate with endoplasmic reticulum (ER) or ER-derived structures (Heinlein et al., 1998; Huang and Zhang, 1999; Kaido et al., 2009; Martínez-Gil et al., 2010; Peremyslov et al., 2004; Verchot-Lubicz et al., 2010). Many experiments have shown that this association of the MP with ER is essential for intra- and inter-cellular movements of virus (Harries et al., 2010; Schoelz et al., 2011). TMV 30K associates with ER-derived inclusion bodies that contain viral replication complexes (VRCs) (Heinlein et al., 1998). TMV 30K is an integral membrane protein and has two transmembrane domains (TMDs) with a topology model in which the N and C termini are exposed to the cytoplasm and there is a short loop in the ER lumen (Brill et al., 2000). There have been relatively few studies of the membrane integration of other MPs belonging to the 30K superfamily, but studies of the MPs of *Prunus necrotic ringspot virus* (PNRSV, genus *Ilarvirus*) and *Red clover necrotic mosaic virus* (RCNMV, genus *Dianthovirus*)

---

* Corresponding authors. Fax: +86 571 8640 4258.
  E-mail addresses: sunliying255@yahoo.com (L. Sun),
jpchen2001@yahoo.com.cn (J. Chen).
  [1] These authors contributed equally to this paper.

showed that their membrane association is not necessarily linked with the TMDs in the same way as TMV 30K. PNRSV MP interacts with the membrane interface through one hydrophobic region thus allowing the N and C termini to be exposed to the cytoplasm (Martínez-Gil et al., 2009) while RCNMV MP localizes to cortical ER through association with a viral replicase complex (Kaido et al., 2009).

MPs appear to utilize distinct intracellular routes for the transport to PD. It is suggested that TMV 30K transports viral RNA to PD along the membrane of the ER/actin network (Kawakami et al., 2004; Wright et al., 2007). Indeed, studies using chemical inhibitors indicate that TMV 30K targets PD without involvement of the ER-to-Golgi secretory pathway (Tagami and Watanabe, 2007; Wright et al., 2007), whereas this pathway is essential for the intracellular transport function of MPs of *Grapevine fanleaf virus* (GFLV, genus *Nepovirus*), *Potato leafroll virus* (genus *Polerovirus*) and *Melon necrotic spot virus* (genus *Carmovirus*) (Genovés et al., 2010; Laporte et al., 2003; Vogel et al., 2007).

Chinese wheat mosaic virus (CWMV) is one of the several members of the genus *Furovirus* (family *Virgaviridae*) which infect cereal plants worldwide (Diao et al., 1999). These viruses have a bipartite, positive sense, single-stranded RNA genome. RNA1 encodes three proteins, two involved in viral replication and a third that is a 37 kDa putative MP (37K). The 19 kDa major coat protein (CP), a 84 kDa minor coat protein and a 19 kDa small cysteine-rich protein (19K CRP) are encoded on RNA2 (Diao et al., 1999). The 37K proteins of furoviruses belong to the 30K super-family of viral MPs (An et al., 2003; Melcher, 2000). In the type member of the genus, *Soil-borne wheat mosaic virus* (SBWMV), the 37K was shown to move to adjacent cells (An et al., 2003) and was able to restore the systemic spread of a TMV vector that had a deletion in the MP coding region (Zhang et al., 2005). CP was not required for the cell-to-cell movement of SBWMV (Miyashita and Kishino, 2010) suggesting that furoviruses move in the form of a vRNP complex.

In this study, the virus movement function of CWMV 37K was confirmed by a *trans*-complementation experiment using a movement-defective *Potato virus X* (PVX) mutant. We then demonstrate that 37K associates with ER-derived vesicles and targets PD. Mutational analysis reveals that two putative TMDs are important for the movement function and subcellular targeting of 37K. We also provide evidence for the involvement of the ER-to-Golgi secretory pathway in intracellular trafficking of 37K. In addition, the interaction of 37K with cellular proteins was explored.

Results

CWMV 37K trans-complements cell-to-cell spread of movement-defective Potato virus X and increases the size exclusion limit of PD in Nicotiana benthamiana

To assess viral movement function of CWMV 37K, we carried out a viral movement complementation experiment utilizing a movement-defective PVX mutant. PVX is the type species of the genus *Potexvirus*, and its movement is facilitated by TGB proteins (Verchot-Lubicz et al., 2010). Previously, cell-to-cell movement of a PVX mutant containing a frame shift mutation in TGBp1 (P25) gene was complemented when co-bombarded with P25 or other viral MPs (Morozov et al., 1997). We introduced a similar frame-shift mutation into the TGBp1 gene of a binary vector based-PVX vector (Lu et al., 2003) carrying the GFP gene. This mutation resulted in a premature stop codon and removed the C-terminal 72 amino acids of P25 (Fig. 1A). An *Agrobacterium* culture harboring PVX-(P25fs)–GFP was diluted 10,000-fold so that
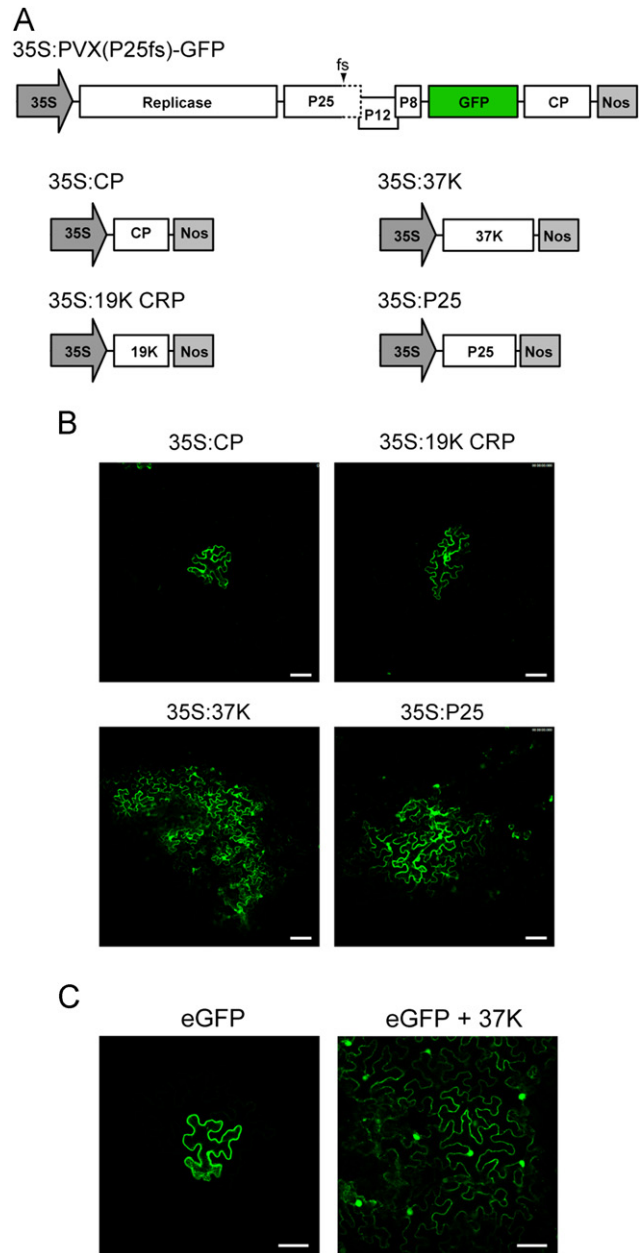

Fig. 1. The ability of CWMV 37K to *trans*-complement cell-to-cell movement of PVX mutants and to increase the size exclusion limit (SEL) of plasmodesmata in *N. benthamiana* plants. (A) A schematic representation of constructs used in the trans-complementation assay (not to scale). An arrowhead marks the position of a frame shift (fs) introduced into PVX P25. 35S and Nos represent cauliflower mosaic virus (CaMV) 35S promoter and nopaline synthase terminator sequences, respectively. (B) *Trans*-complementation assay of the movement of PVX mutant. An *Agrobacterium* culture harboring 35S:PVX(P25fs)–GFP was diluted 10,000-fold and mixed (1:1:1) with two Agrobacterium cultures harboring 35S:p19 and 35S:CP, 35S:19K CRP, 35S:37K or 35S:P25. The mixtures were infiltrated into leaves of *N. benthamiana* and GFP fluorescence was observed using confocal laser scanning microscopy (CLSM) 5 days post inoculation (dpi). Bars, 75 μm. (C) Ability of 37K to increase the SEL of plasmodesmata. An *Agrobacterium* culture harboring 35S:eGFP was diluted 10,000-fold and mixed (1:1) with an *Agrobacterium* culture harboring 35S:37K to increase the SEL of plasmodesmata. An *Agrobacterium* culture harboring 35S:eGFP was diluted 10,000-fold and mixed (1:1) with an *Agrobacterium* culture harboring 35S:37K. The mixtures were infiltrated into leaves of *N. benthamiana* and the GFP fluorescence was observed using CLSM 3 dpi. Bars, 20 μm.

isolated cells become infected, and mixed with *Agrobacterium* cultures harboring binary expression vectors containing CWMV 37K, PVX P25, CWMV CP or CWMV 19K CRP. An *Agrobacterium* culture harboring a binary expression vector containing the p19 RNA silencing suppressor of *Tomato bushy stunt virus* (genus *Tombusvirus*) was also mixed to each combination of bacterial

cultures to *trans*-complement P25 silencing suppression activity (Bayne et al., 2005). The bacterial mixtures were then used to infiltrate *Nicotiana benthamiana* leaves. The cell-to-cell spread of the PVX mutant as indicated by formation of GFP foci in infiltrated

leaves was observed under long-wave UV light or using confocal laser scanning microscopy (CLSM) 5 days post inoculation (dpi). On the leaves expressing 37K and PVX P25, bright GFP foci were visible with the naked eye under UV light but none was seen on
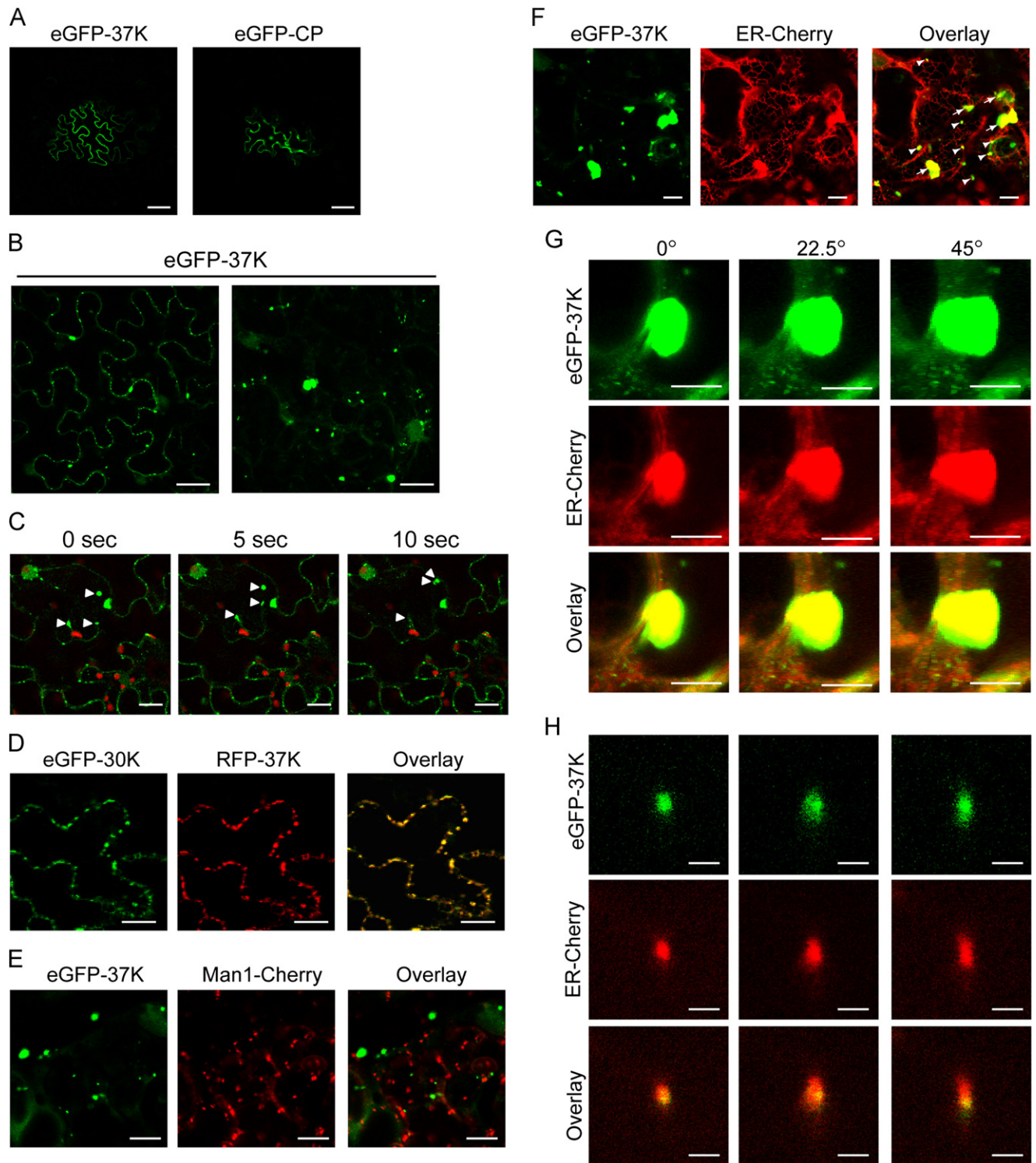

Fig. 2. Subcellular localization of CWMV 37K. (A) Cell-to-cell diffusion of 37K fused to eGFP. An *Agrobacterium* culture harboring eGFP-37K or eGFP-CP was diluted 10,000-fold and infiltrated into leaves of *N. benthamiana*. Fluorescence was observed using CLSM 3 dpi. Bars, 25 μm. (B) Subcellular localization of eGFP-37K in epidermal cells. Bars, 20 μm. (C) Time lapse imaging (consecutive images every 5 s) of epidermal cells expressing eGFP-37K. Arrowheads mark the position of the mobile vesicles. Bars, 20 μm. (D) Co-expression of red fluorescent protein (RFP)-37K with plasmodesmatal marker (eGFP-30K). Bars, 20 μm. (E and F) Co-expression of eGFP-37K with markers for the Golgi apparatus (ManI-Cherry) or ER lumen (ER-Cherry). Bars, 10 μm. (G) Three dimensional (3D) images of a large aggregate structure in cell expressing eGFP-37K and ER-Cherry. The 3D images were generated from the optical cross sections (seven frames) with 1-μm thick single plane images. The rotations were at 0°, 22.5° and 45° along with Y-axis. Bars, 60 μm. (H) Consecutive 1-μm thick single plane images (from left to right) of a small vesicular structure in cell expressing eGFP-37K and ER-Cherry. Bars, 20 μm.

the leaves expressing CWMV CP or 19K CRP (data not shown and see also Fig. 5A). In CLSM of the leaves expressing CWMV CP or 19K CRP, GFP expression was confined to single cells whereas leaves expressing 37K or PVX P25 had most of the GFP expressed in clusters of cells (Fig. 1B). This result indicates that 37K is able to *trans*-complement the cell-to-cell movement of PVX-(P25fs)–GFP. Next we tested the ability of 37K to increase the size exclusion limit (SEL) of PD by examining the effect of 37K expression on cell-to-cell diffusion of enhanced green fluorescent protein (eGFP). When an *Agrobacterium* culture harboring 35S:eGFP was highly diluted (10,000-fold) and expressed alone, eGFP expression was restricted to a single cell. In contrast, co-expression with 37K enabled eGFP cell-to-cell diffusion throughout the mesophyll cells of infiltrated leaves (Fig. 1C), which is probably due to the increase in SEL of plasmodesmata. Taken together, these results strongly suggest that CWMV 37K is a viral MP.

CWMV 37K localizes to plasmodesmata and ER-derived structures

To analyze 37K subcellular localization, 37K was fused to the C-terminus of eGFP (eGFP-37K) and transiently expressed in leaves of *N. benthamiana* plants by agroinfiltration. eGFP expression in epidermal cells was observed by CLSM 3 dpi. First we utilized the fluorescent fusion protein to examine the ability of 37K to move to adjacent cells. When the *Agrobacterium* culture harboring the eGFP-37K construct was highly diluted (10,000-fold), most of the green fluorescence was observed in clusters of 3 to 4 cells, in which a single bright green fluorescent cell was surrounded by 2 to 3 cells with faint fluorescence. In contrast, eGFP-CP expression was clearly confined to a single cell (Fig. 2A). This observation indicates that 37K is able to move to adjacent cells similar to previously demonstrated for 37K of SBWMV (An et al., 2003).

CLSM observation of epidermal cells expressing eGFP-37K showed that the fusion protein accumulated in stationary punctate spots along the cell periphery (Fig. 2B, left panel), a characteristic of PD localization. To confirm this, 37K was fused to red fluorescent protein (RFP-37K) and co-expressed with eGFP fused to TMV 30K (eGFP-30K), which is known to localize in PD (Tomenius et al., 1987). RFP-37K was co-localized with eGFP-30K in the punctate spots along the cell periphery (Fig. 2D), confirming that 37K localized to PD. eGFP-37K also accumulated in numerous small vesicular structures distributed throughout the cells and to a lesser extent in large aggregate bodies with sizes ranging from 0.3 to 1.0 μM (Fig. 2B, right panel). Time-lapse imaging revealed that many of the small vesicular structures were mobile whereas the large aggregate bodies remained stationary or moved only slightly (Fig. 2C). Many of the small structures moved toward or along the cell periphery. No green fluorescence was observed in the cortical ER network. eGFP-37K consistently showed localization to PD and small vesicular structures in almost all of the observed cell (up to 80 cells), whereas the presence of large aggregate structures were observed only in about 70% of the cells. To further investigate the nature of these structures, eGFP-37K was co-expressed with Golgi- and ER-specific markers. ManI-Cherry, which contains a signal targeted to the Golgi apparatus, associated with mobile vesicles but none of them overlapped with the structures formed by eGFP-37K (Fig. 2E), suggesting that 37K does not localize in the Golgi apparatus. The ER luminal marker (ER-Cherry) localized in the cortical ER network and interestingly, also accumulated in large aggregates that co-localized with eGFP-37K-induced structures (Fig. 2F, arrows). When ER-Cherry was expressed alone, red fluorescence was observed in the cortical ER but there were none of the large aggregate structures that had been observed using eGFP-37K (data not shown). Similarly, most of the eGFP-37K-induced small vesicular structures also overlapped with vesicular structures

formed by ER-Cherry or aligned with ER tubules (Fig. 2F, arrowheads). To further examine the relationship of eGFP-37K-induced structures with ER, a three dimensional (3D) image of large aggregate structures was generated from optical cross sections. The 3D construction revealed that eGFP-37K and ER-Cherry completely overlapped when rotated along Y-axis (Fig. 2G). In addition, consecutive optical cross sections (1-μm thick) of the small vesicular structure also showed that red fluorescence overlapped with the green fluorescence (Fig. 2H). These observations suggest that the eGFP-37K-induced structures are derived from ER membranes.

Two putative transmembrane domains in the N-terminal half are important for CWMV 37K activity and subcellular localization

Because of the association of 37K with ER (Fig. 2F), we analyzed the 37K sequence for potential TMDs. Hydrophobicity
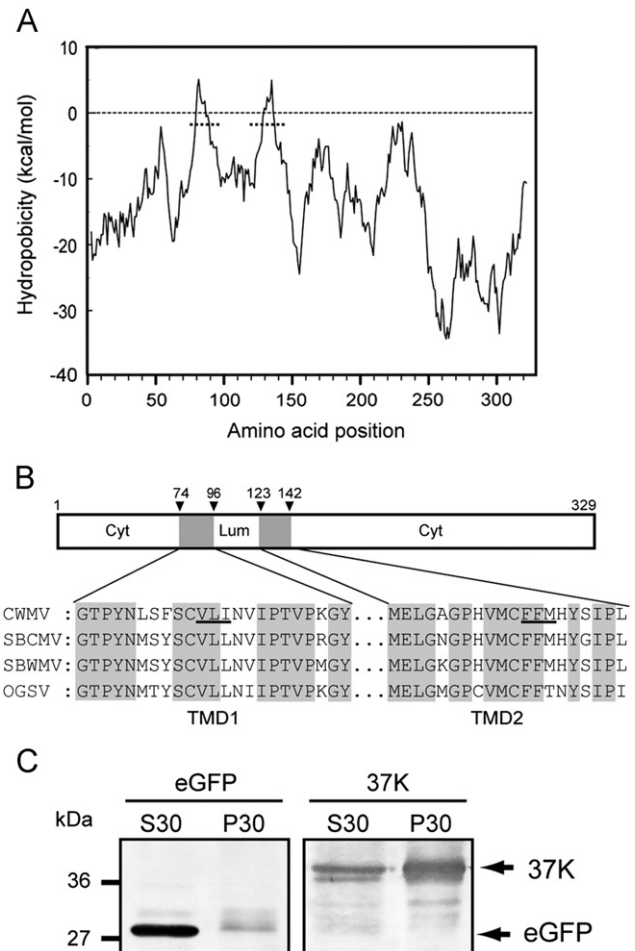

Fig. 3. Hydrophobic profile and transmembrane domains of CWMV 37K. (A) Hydrophobic plot of 37K generated with MPEx according to the Wimley and White octanol hydrophobicity scale. The plot shows the mean values using a window of 19 residues. Dashed lines indicate the predicted hydrophobic regions. (B) A schematic map showing the position of two transmembrane domains (TMD1 and TMD2) in 37K as predicted by TMpred. Cyt and Lum indicate the cytoplasmic and luminal domains, respectively. Amino acid sequences of transmembrane domains of CWMV 37K and the corresponding sequences in 37K of other furoviruses are presented. Gray boxes indicate that amino acids are identical. Amino acids that were substituted to proline are underlined. SBCMV: *Soil-borne cereal mosaic virus*, SBWMV: *Soil-borne wheat mosaic virus*, OGSV: *Oat golden stripe virus*. (C) Association of CWMV 37K with cellular membranes. *N. benthamiana* leaves transiently expressing 37K or eGFP were homogenized and then subjected to differential centrifugation. The presence of 37K or eGFP in the soluble fraction (S30) and crude membrane containing fraction (P30) was detected by Western blot using 37K and GFP-specific antisera.

analysis using the algorithm developed by Wimley and White (1996) revealed that two short hydrophobic regions exist in the N-terminal half of the protein (Fig. 3A). In the transmembrane protein prediction programs TMpred and TopPred II, those hydrophobic regions (amino acids position 74–96 and 123–142) were predicted to be TMDs (TMD1 and TMD2) with a topology in which the N- and C-termini are located in the cytoplasm (Fig. 3B). Sequence analyses of the 37K encoded by other furoviruses showed that a similar hydrophobic and highly conserved regions occur in SBWMV, *Soil-borne cereal mosaic virus* and *Oat golden stripe virus* (Fig. 3B). In a fractionation experiment using the *N. benthamiana* leaves transiently expressing 37K or eGFP, 37K was mostly associated with the crude membrane fraction whereas the control eGFP was associated with the soluble fraction (Fig. 3C). This result further confirmed the association of 37K with cellular membranes.

To examine the importance of TMDs for 37K function, we generated two mutants that contained amino acid substitutions in either TMD1 or TMD2. Mutations were designed to reduce the hydrophobicity of the TMD. Valine, leucine and isoleucine (VLI) at amino acid position 84–86 in the TMD1 and two phenylalanine and methionine (FFM) at amino acid position 134–136 in the TMD2 (Fig. 3B) were substituted to three consecutive prolines (hydrophilic amino acid) to produce mTM1 and mTM2 mutants

(Fig. 4A). In addition, we constructed four 37K deletion mutants that deleted either the N-terminal (dN1 and dN2) or C-terminal regions (dC1 and dC2) (Fig. 4A). All of the mutants were then tested for their ability to complement cell-to-cell movement of the PVX mutant in agro-coinfiltration as described above. At 5 dpi, bright GFP foci were seen under UV light in leaves expressing wild type 37K but not in leaves expressing the dC1 and other 37K mutants (Fig. 5A and data not shown). However, when observed using CLSM, GFP expression was spread in the epidermal cells of leaves expressing the dC1 mutant, whereas with the mTM1, mTM2 and other mutants GFP expression was confined to a single cell (Fig. 5B and data not shown). Next we did further analyses to determine whether the dC1 mutant is able to promote the spread of the PVX mutant or only the cell-to-cell diffusion of GFP. By western blot analysis, a high level of GFP accumulation was detected in leaves expressing 37K but very low levels or none in leaves expressing the dC1 mutant or mTM1 (Fig. 5C). Next, total RNAs were extracted from infiltrated leaves and PVX RNA accumulation was detected by RT-PCR using PVX CP- specific and oligo (dT) primers. PVX RNA was detected in leaves expressing 37K but not in leaves expressing the dC1 mutant or mTM1 (Fig. 5D). These analyses suggest that the dC1 mutant is unable to complement cell-to-cell movement of PVX mutant but still retains the ability to increase the SEL of PD.
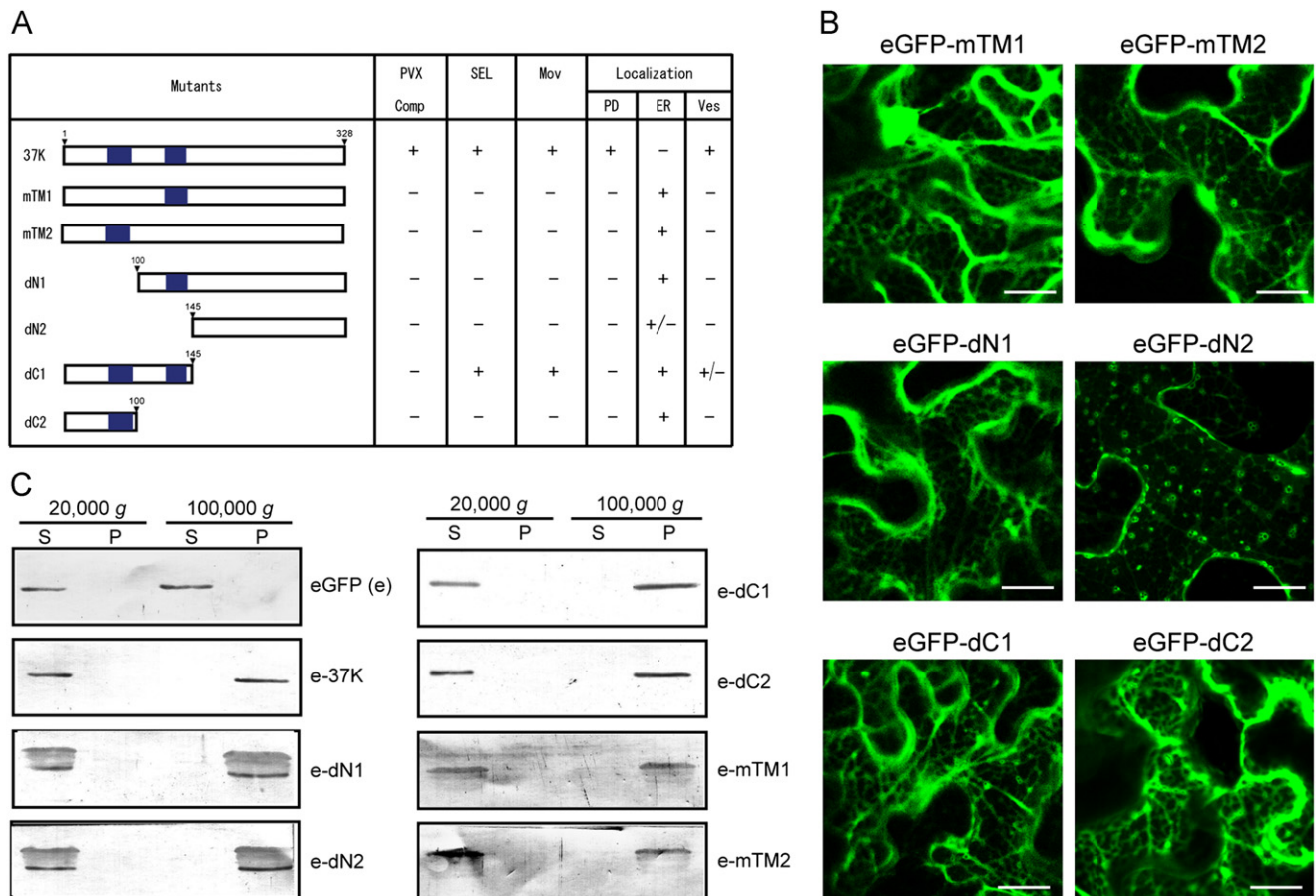

Mutants	PVX Comp	SEL	Mov	Localization		
				PD	ER	Ves
37K	+	+	+	+	−	+
mTM1	−	−	−	−	+	−
mTM2	−	−	−	−	+	−
dN1	−	−	−	−	+	−
dN2	−	−	−	−	+/−	−
dC1	−	+	+	−	+	+/−
dC2	−	−	−	−	+	−

Fig. 4. The roles of the transmembrane domains in the movement function and subcellular localization of CWMV 37K. (A) A schematic representation of 37K mutants and a summary of the results obtained from the *trans*-complementation assay (PVX Comp), the plasmodesmata gating assay (SEL), observation of cell-to-cell movement of fusion proteins (Mov) and the subcellular localization to plasmodesmata (PD), endoplasmic reticulum network (ER), or vesicular structures (Ves). Blue boxes represent the transmembrane domains. The amino acid positions of the N-or C-terminal ends of deletion mutants in the 37K sequence are indicated above the arrowhead. (+), (−) and (+/−) indicate ability, inability and low ability, respectively. (B) Subcellular localization of 37K mutants fused to eGFP in epidermal cells. EGFP fluorescence was observed using CLSM 3 dpi. Bars, 20 μm. (C) A fractionation experiment to examine the association of eGFP fusion proteins with cellular membranes. Protoplast isolated from the *N. benthamiana* leaves transiently expressing the eGFP fusion proteins were homogenized and then subjected to differential centrifugation. The presence of eGFP fusion proteins in the soluble fractions (20,000*g* supernatant (S)) and microsomal fraction (100,000*g* pellet (P)) was detected by Western blot using GFP-specific antiserum. (For interpretation of the references to color in this figure legend, the reader is referred to the web version of this article.)
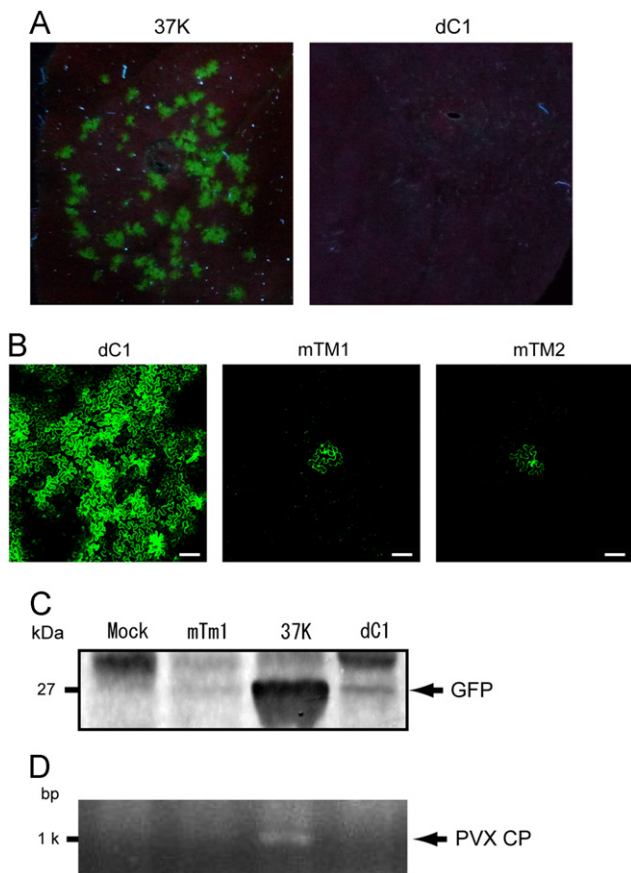
Fig. 5. *Trans*-complementation assay assessing the ability of CWMV 37K mutants to recover the movement of a PVX mutant. (A and B) GFP expression in leaves used for the *trans*-complementation assay. An *Agrobacterium* culture harboring 35S:PVX(P25fs)–GFP was diluted 10,000-fold and mixed (1:1:1) with two *Agrobacterium* cultures harboring 35S:p19 and wild-type or mutants of 37K. The mixtures were infiltrated into leaves of *N. benthamiana* and the GFP fluorescence was observed 5 dpi under UV light (A) or using CLSM (B). Bars, 100 μm. (C) Western blot analysis to detect GFP accumulation in leaves used for the *trans*-complementation assay described in A. (D) RT-PCR analysis to detect PVX RNA accumulation in leaves used for the *trans*-complementation assay described in A.

To examine the effect of mutation or deletion on 37K subcellular localization, all of the mutants were fused to eGFP and transiently expressed in leaves. First, in an experiment when the bacterial cultures were highly diluted (10,000-fold), the expression of eGFP fused to dC1 was observed in clusters of 2–4 cells whereas the other mutants remained in single cells (Supplementary Fig. 1), Thus the PD gating activity of the dC1 mutant allows diffusion of fusion protein into adjacent cells. CLSM observation showed that none of the fusion proteins accumulated in punctate spots along the cell periphery, suggesting that they no longer associate with PD. The accumulation of eGFP fused to mTM1, mTM2, dN1, dC1 or dC2 was clearly visible in the cortical ER network and oftenly aggregates at the vortexes of ER networks to form ring-like structures, while eGFP-dN2 faintly labeled ER network but strongly localized to ring-like structures at ER vortexes (Fig. 4B). Motile vesicular structures were rarely seen in cells expressing eGFP-dC1 and never observed in cells expressing eGFP fused to other mutants (data not shown). To further confirm the association of fusion proteins with cellular membranes, a fractionation experiment using the protoplast isolated from the *N. benthamiana* leaves transiently expressing the fusion proteins was carried out. The results showed that eGFP fused with 37K or mutants but not unfused eGFP was associated with microsomal fractions (100,000*g*

pellet) (Fig. 4C). In summary, mutational and deletion analyses provide evidence that both predicted TMDs are important for movement activity and subcellular localization of 37K.

Intracellular transport of CWMV 37K Is dependent on the ER-to-Golgi secretory pathway

The role of the secretory pathway in the intracellular trafficking of 37K was investigated using chemical and protein inhibitors. Brefeldin A (BFA) is a fungal toxin known to inhibit the ADP-ribosylation guanine nucleotide exchange factor (ARF–GEF) leading to inhibition of vesicle trafficking along the secretory pathway (Nebenführ et al., 2002) while Sar1[H74L] is a dominant-negative mutant of the Ras-like small GTPase (Sar1p) that specifically inhibits COPII-mediated ER-to-Golgi transport (Robinson et al., 2007). eGFP-37K was co-expressed with a Golgi marker (ManI-Cherry) to monitor the effect of treatments. Infiltration of leaves with BFA led to accumulation of eGFP-37K in the cortical ER network (Fig. 6A). The large aggregate bodies were still observed but the small vesicular structures were drastically reduced when compared to non-treated leaves. EGFP-37K localization to PD was still seen although to a lesser extent (Fig. 6A, left image), which may be due to transport to PD before BFA treatment. BFA treatment also resulted in accumulation of ManI-Cherry in the cortical ER but less in the Golgi stack, indicating that the protein was reabsorbed into the ER. It was also observed that ManI-Cherry co-localized with the large aggregates formed by eGFP-37K (Fig. 6A, arrow). When Sar1[H74L] was co-expressed, both proteins evidently remained in the cortical ER (Fig. 6B). Vesicular and large aggregates structures were not observed and eGFP-37K accumulation in PD was hardly seen (Fig. 6B, left image). Together, these results indicate that ER export and intracellular transport of 37K to PD are dependent on the early secretory pathway.

Microfilaments have been implicated in the intracellular transport of viral MPs (Genovés et al., 2010; Haupt et al., 2005; Ju et al., 2005; Kawakami et al., 2004). We examined the effect of disruption of actin filaments on 37K subcellular distribution by treatment with latrunculin B (LatB), an actin-depolymerizing drug. The treatment resulted in accumulation of eGFP-37K in large compartments, resembling the secretion of protein in apoplastic space (Fig. 6C). However, plasmolysis of the leaf tissue showed that those compartments were retracted with the protoplast (data not shown), indicating that eGFP-37K remained inside the cytoplasm. As expected, LatB treatment resulted in disappearance of the actin network in RFP-Talin expressing leaves (Fig. 6C). In a control experiment when leaves were infiltrated with dimethyl sulfoxide (DMSO), no effect was observed (Fig. 6C). These observations suggest that the intact actin cytoskeleton is important for the proper subcellular distribution of 37K.

CWMV 37K interacts with pectin methylesterases

The interactions of MP (30K) of tobamoviruses with cellular proteins have been reported by several studies. Aside from interaction with cytoskeletal proteins, TMV 30K interacts with an ankyrin repeat-containing protein 1 (ANK1), pectin methylesterases (PME), calreticulin 1 (CRT1) and DnaJ-like proteins (MPIP1) (Chen et al., 2000; Chen et al., 2005; Heinlein et al., 1995; McLean et al., 1995; Shimizu et al., 2009; Ueki et al., 2010). Using a bimolecular fluorescence complementation (BiFC) assay (Hu and Kerppola, 2003), we investigated whether 30K and 37K share common host interactor proteins. The CWMV 37K and TMV 30K genes were fused to the N-terminal portion of yellow fluorescent protein (NYFP) that had been inserted into a binary vector and the full length open reading frames (ORFs) of
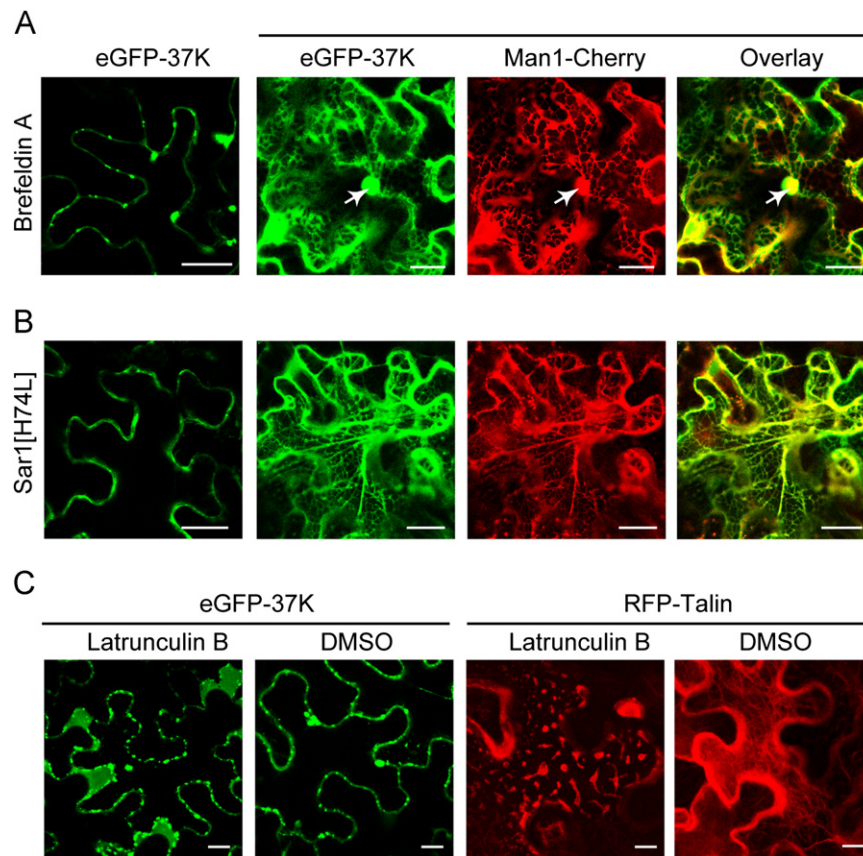
Fig. 6. The effects of Brefeldin A, Sar1[H74L] and Latrunculin B on the subcellular localization of CWMV 37K. (A) Leaves co-expressing eGFP-37K and ManI-Cherry (Golgi marker) were infiltrated with 10 µg mL^{-1} Brefeldin A. Fluorescent proteins were observed using CLSM 3 dpi. Arrows mark the co-localization of ManI-Cherry with 37K-induced aggregate structures. Bars, 25 µm. (B) eGFP-37K and ManI-Cherry were co-expressed with Sar1[H74L]. Bars, 25 µm. (C) The leaves expressing eGFP–37K or RFP-Talin were infiltrated with 50 µg mL^{-1} Latrunculin B or DMSO as a control. Bars, 10 µm.

N. tabacum ANK1, *N. tabacum* MPIP1, *N. benthamiana* PME and *A. thaliana* CRT1 were fused to the C-terminal portion of YFP (CYFP). The resulting plasmids were transformed into *Agrobacterium* and used to co-infiltrate *N. benthamiana* leaves. The reconstruction of YFP fluorescence indicating a protein-protein interaction was visualized using CLSM 3 dpi. Bright YFP fluorescence was observed in leaves infiltrated with *Agrobacterium* harboring NYFP-30K plus *Agrobacterium* harboring CYFP–Nt–ANK1, CYFP–Nt–MPIP1, CYFP–Nb–PME or CYFP–At–CRT1 (Fig. 7A). When interactions of these proteins with 37K were tested, only the combination with Nb–PME exhibited bright YFP fluorescence (Fig. 7A). In a negative control experiment, interaction of CWMV CP with 30K-interactor proteins or 37K was not observed (Fig. 7A and data not shown). Interaction of 37K and Nb–PME was further confirmed using a yeast two-hybrid assay. The 37K fused to the activation domain showed interaction with Nb–PME fused to the DNA binding domain (Fig. 7B). Because PME is a cell wall-associated protein (Chen et al., 2000), we plasmolyzed epidermal cells expressing NYFP-37K and CYFP–Nb–PME. During plasmolysis significant amounts of YFP fluorescence remain anchored to the cell wall and did not incorporate into the retracting protoplast (Fig. 7C, arrowheads), showing that the interaction of 37K and Nb–PME occurs in the cell wall. Similar results were observed when leaves expressing NYFP-30K and CYFP–Nb–PME were treated by plasmolysis (data not shown). Interaction of six 37K mutants (Fig. 4A) with Nb–PME was also assayed by BiFC. Analysis showed that only mutant dN2 interacted with Nb–PME (Fig. 7D and data not shown), suggesting that the C-terminal half of 37K is responsible for the interaction with Nb–PME . Because mutants dN1, mTM1 and mTM2 did not

interact with Nb–PME , it seems that the removal of one of the TMDs abolishes the interaction of 37K with Nb–PME *in planta*.

Discussion

Although CWMV usually infects only wheat plants in the field, we found that it can also infect *N. benthamiana* through foliar-rub inoculation and spreads systemically to the upper leaves (unpublished result). Thus *N. benthamiana* is an appropriate plant system for studying the movement function and subcellular localization of 37K. Since infectious cDNA clones for reverse genetic analysis of CWMV are still unavailable, we investigated the movement function of 37K by a heterologous system using a movement-defective PVX mutant in *N. benthamiana* leaves (Fig. 1). Previous studies have demonstrated that the *trans*-complementation assay using movement-defective PVX is reliable for assessing the movement function of diverse viral MPs. The cell-to-cell spread of a TGBp1-defective PVX mutant was restored when co-bombarded with plasmids expressing MPs of *Tomato mosaic virus*, Crucifer tobamovirus or RCNMV (Morozov et al., 1997). The same PVX mutant has been utilized to identify MPs of *Rice dwarf virus* (genus *Phytoreovirus*) and *Rice stripe virus* (genus *Tenuivirus*), two viruses that infect monocotyledonous plants (Li et al., 2004; Xiong et al., 2008).

Our experiments showed that CWMV 37K possesses the common characteristics of a viral movement-associated protein, including the ability to increase SEL (Fig. 1C), movement to adjacent cells (Fig. 2A) and localization to PD (Fig. 2B and D). An eGFP-37K fusion protein associated with two kinds of
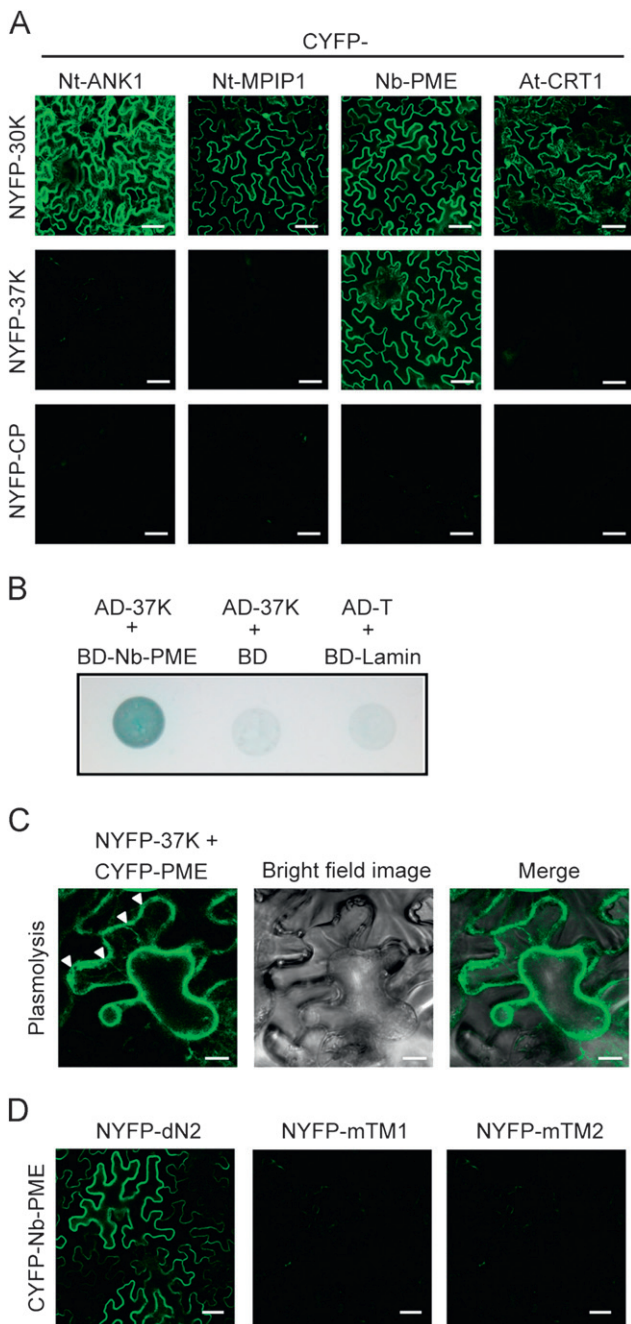
Fig. 7. Interaction of CWMV 37K with cellular proteins. (A) BiFC assay to examine the interaction of TMV 30K or 37K with a *N. tabacum* ankyrin repeat-containing protein (Nt–ANK1), *N. benthamiana* pectin methylesterase (Nb–PME), *A. thaliana* calreticulin (At-CRT1) and *N. tabacum* DnaJ-like protein (Nt–MPIP1). Leaves of *N. benthamiana* were infiltrated with the mixtures of an *Agrobacterium* culture harboring constructs indicated above and on the left side of the images. YFP fluorescence was observed using CLSM 3 dpi. Bars, 60 μm. (B) Yeast two-hybrid assay to test the interaction of 37K with Nb–PME. The 37K was fused to the Gal4 activation domain (AD-37K) and Nb-PME was fused to the Gal4 DNA-binding domain (BD–Nb–PME). Yeast cells harboring constructs were grown on selective medium lacking histidine, leucine, tryptophan and adenine and supplemented with X-α-Gal. Large T-antigen (T) and Lamin were included in the assay as negative controls. (C) Plasmolysis of leaves expressing NYFP-37K and CYFP–Nb–PME described in A. Arrowheads mark the position of YFP fluorescence that remained in the cell wall. Bars, 10 μm. (D) BiFC assay to examine the interaction of Nb–PME with 37K mutants. Bars, 45 μm.

structure in the cytoplasm, the mobile vesicular and the large aggregate structures (Fig. 2B and C). In co-localization experiment, these structures were co-localized with an ER marker but not with a marker for the Golgi apparatus (Fig. 2E and F), which suggest that both kinds of structure were derived from ER membranes. The large aggregate structures induced by 37K resemble the aggregate structures formed by TMV 30K through conversion of tubular ER (Reichel and Beachy, 1998). Many vesicles were observed to move toward, or traverse along, the cell periphery and are therefore probably the membrane-bound vesicles that are involved in transporting 37K to the PD or cell surface. Vesicular structures are also induced by membrane-associated MPs belonging to the TGB family (Verchot-Lubicz et al., 2010). For example, TGBp2 and TGBp3 of *Potato mop-top virus* (PMTV, genus *Pomovirus*) show early association with the cortical ER network and eventually associate with mobile granular-like structures (Haupt et al., 2005; Tilsner et al., 2010) while TGBp2 of PVX simultaneously associated with ER and with mobile ER-derived vesicles (Ju et al., 2005). PMTV TGBp2 and TGBp3-induced granular structures are thought to facilitate the transport of the viral RNA complex to and through PD along the ER-actin network (Haupt et al., 2005). Supporting this proposal, PVX TGBp2-induced vesicles appear to be important for virus movement (Ju et al., 2007). TMV 30K associates with the VRC (Heinlein et al., 1998) and, similarly, recent studies have shown co-localization of PVX TGBp3 and RCNMV MP with the replicase in ER-derived structures (Bamunusinghe et al., 2009; Kaido et al., 2009). Future studies will be focused on investigating whether 37K-induced structures associate with the VRC and are involved in intracellular transport of viral RNAs to PD.

Amino acid mutations that disrupt the hydrophobicity of either TMD1 or TMD2 (mTM1 or mTM2 mutants) abolished the ability of 37K to complement cell-to-cell spread of the PVX mutant (Fig. 5). Those mutations also resulted in the retention of eGFP-37K in the cortical ER network and prevented PD localization and the formation of ER-derived structures (Fig. 4). These results provide evidence that ER export and the formation of ER-derived vesicles are important for the movement function of 37K. Export of the transmembrane protein from the ER is a selective process and requires transport signals or motifs that are recognized by coat subunits of COPII (Aridor et al., 1998; Barlowe, 2003). These ER export signals are usually present in the cytosolic domain of transmembrane proteins (Barlowe, 2003; Cai et al., 2011). The predicted topology model of 37K (Fig. 3B) seems plausible since the N-and C-terminal domains which may be important for ER export or other functions are exposed to the cytoplasm. Thus, disruption of either of the TMDs may alter the topology of 37K and cause one of the termini to reside in the ER lumen. This probably explains why most of the 37K mutants remained in the ER (Fig. 4B). Deletion of the C-terminal region (dC1) resulted in ER retention despite the presence of both TMDs (Fig. 4), which may suggest that the C-terminal domain contains an ER export signal. The di-acidic or di-hydrophobic ER export motifs found in some type-I transmembrane proteins (Barlowe, 2003) are not present in the C-terminal domain of 37K and further study is therefore needed to characterize the ER export signals of 37K. Interestingly, the dC1 mutant still retained the ability to increase SEL (Fig. 5), demonstrating that ER export and PD targeting of 37K are not critical for PD gating activity. In summary, this study revealed a substantial difference between the intracellular route of CWMV 37K and that of TMV 30K. CWMV 37K transport to PD requires ER export and formation of transport vesicles that depend on the early secretory pathway (Fig. 6B). In contrast, TMV 30K transport to PD is independent of the secretory pathway and cell-to-cell movement of TMV is not affected by inhibition of the secretory pathway (Genovés et al., 2010; Tagami and Watanabe, 2007; Wright et al., 2007). One study proposes that the TMV 30K-associated VRC transports from the replication site to the PD by diffusion within the ER lipid to

the desmotubule (Guenoune-Gelbart et al., 2008). Different requirements for the secretory pathway were also observed between two tubule-forming MPs belonging to the 30K super-family. PD targeting of Cowpea mosaic virus (genus Comovirus) MP does not involve the secretory pathway whereas the intracellular trafficking of the MP of GFLV to PD is dependent on the secretory pathway (Laporte et al., 2003; Pouwels et al., 2002).

To facilitate viral cell-to-cell movement, the MP needs to cooperate with diverse cellular factors (Boevink and Oparka, 2005). Among several TMV 30K-interactor proteins tested in this study, Nb-PME was found to interact with 37K (Fig. 7). PME is a cell wall-associated protein that has roles in cell wall metabolism and plant morphology (Chen et al., 2000; Hongo et al., 2012). A previous report showed that the MPs of Turnip vein clearing virus (genus Tobamovirus) and Cauliflower mosaic virus (genus Caulimovirus) also bind PME (Chen et al., 2000). Thus, PME may be the cellular protein that is generally targeted by MPs of the 30K superfamily. A TMV 30K mutant defective in interaction with PME was unable to facilitate cell-to-cell spread of TMV, suggesting that the association of TMV 30K with PME is important for TMV movement (Chen et al., 2000). Moreover, suppression of PME expression in the vascular tissue of transgenic tobacco plants delays the systemic movement of TMV (Chen and Citovsky, 2003). We determined that the C-terminal region of 37K contributes to its interaction with PME while mutation or deletion of one of the TMDs disrupted the interaction in planta (Fig. 7D). This is possibly due to inability of those mutants to target the cell wall. It has been suggested that the activity of PME may be affected by binding to TMV 30K, which in turn changes PD permeability (Chen et al., 2000). The dC1 mutant still exhibited PD gating activity although it did not interact with PME, suggesting that interaction with PME is not crucial for PD gating activity of 37K. Nevertheless, it remains possible that the interaction of 37K with PME is important for CWMV movement.

Materials and methods

Plant materials

N. benthamiana plants were grown in soil and kept in a growth cabinet at 22 °C for 16 h in daylight.

RNA extraction and RT-PCR

Total RNA was extracted by Trizol (Invitrogen) according to the manufacturer's protocol. First strand cDNAs were synthesized using ReverTra Ace reverse transcriptase (Toyobo) and PCR amplified using Blend Tag DNA polymerase (Toyobo) according to the manufacturer's protocols. The CWMV 37K, CP and 19K CRP genes were amplified by RT-PCR using total RNA extracted from leaves of wheat plants infected with CWMV isolate Rongcheng (Yang et al., 2001). TMV 30K was derived from TMV isolate OM (Ohno et al., 1984). The full length ORFs of N. tabacum ANK1 (accession no. AAO91861), N. benthamiana PME (accession no. AY238968), A. thaliana CRT1 (accession no. NM_104513) and N. tabacum MPIP1 (accession no. AB092334) were amplified by RT-PCR . Site-directed mutagenesis of 37K was carried out by two PCR steps as described previously (Herlitze and Koenen, 1990). Primer sequences used in this study are available upon request.

Plasmid constructs

For transient gene expression, DNA fragments were ligated into the binary vector pBin61 (Voinnet et al., 1998) between BamHI and SmaI sites. To prepare fluorescent protein fusions, the eGFP or RFP gene was first inserted between the XbaI and BamHI sites of pBin61. DNA fragments were then inserted between the BamHI and SmaI sites of pBin-eGFP or pBin-RFP . For the BiFC assay, DNA fragments corresponding to amino acids 1–174 and 175–239 of the YFP gene were inserted between the XbaI and BamHI sites of pBin61. Subsequently, DNA fragments were inserted between the BamHI and SmaI restriction sites located downstream of the N-terminal or C-terminal portions of the YFP gene in pBin-NYFP and pBin-CYFP plasmids.

To construct PVX with a mutated P25 (TGBp1) gene, plasmid pGR106 (Lu et al., 2003) was digested with Bsp1201, blunt-ended by Klenow enzyme and re-ligated . Sequence analysis showed that this treatment introduced four extra nucleotides which resulted in a codon frame shift and a premature internal stop codon. For expression of recombinant proteins in E. coli, the 37K ORF was introduced between the BamHI and NotI sites of pGEX-6P-1 (Invitrogen). For the yeast two-hybrid assay, 37K and Nb-PME ORF were inserted into the BamHI-SmaI sites of pGADT7 and pGBKT7 (Clontech), respectively.

The pBin-p19 and pBin-P25 (Voinnet et al., 2000,2003) were kindly provided by David Baulcombe (Cambridge University, UK). The fluorescent organelle markers ManI-Cherry, ER-Cherry and RFP-Talin have been described previously (Kost et al., 1998; Nelson et al., 2007). The plasmid Sar1[H74L] mutant (Wei and Wang, 2008) was generously provided by Taiyun Wei.

Agrobacterium infiltration

For Agrobacterium infiltration, plasmid constructs were trans-formed into Agrobacterium tumefaciens strain C58C1 and then used to infiltrate N. benthamiana leaves as described previously (Voinnet et al., 1998). The PVX vector mutant plasmid was transformed into A. tumefaciens strain GV3101 and used to infiltrate N. benthamiana leaves.

CWMV 37K antiserum production

GST-tagged 37K was expressed in E. coli strain BL21 (Novagen) and purified using methods described previously (Sun and Suzuki, 2008). Protein was diluted in a buffer containing 50 mM Tris-HCl (pH 8.0), 75 mM NaCl and 1 × protease inhibitor cocktail (Roche) and emulsified with Freund's incomplete adjuvant (Difco). Antigen (1 mg ml^{-1}) was subcutaneously injected into New Zealand white rabbits. Antiserum was produced by Shengong Biotech Co. Ltd. (Shanghai, China).

Subcellular fractionation

Leaves (5 g) were homogenized in 10 ml buffer H containing 20 mM Tris-HCl (pH 8.0), 200 mM NaCl, 1 mM EDTA and 1 × protease inhibitor cocktail (Roche). The homogenate was centrifuged twice at 1,000g for 15 min to remove chloroplast, cell wall and debris. The supernatant was centrifuged at 30,000g for 30 min to obtain soluble (S30) and crude membrane fractions (P30). For fractionation experiment using protoplast, leaves were transversally incised to generate a fine comb and soaked in an enzyme solution containing 0.6 M mannitol, 10 mM CaCl$_2$ (pH 5.6) and 1% cellulose (Onozuka R-10) and 0.05% Macerozyme (both from Yakult Honsha CO., Japan) for 4 h at 30 °C in the dark. Protoplast were put through a 64-mesh sieve and collected by centrifugation at 500g for 10 min. Washing (three times) was performed in a solution containing 0.6 M mannitol, 10 mM CaCl$_2$ (pH 5.6). Protoplast were homogenized in buffer H and then subjected to differential centrifugation at 20,000g and 100,000g to obtain soluble and microsomal fractions, respectively.

Western blot analysis

Preparation of protein samples, SDS-PAGE, electroblotting and immunodetection were carried out as described previously (Sun and Suzuki, 2008). CWMV 37K was detected using primary anti-37K polyclonal serum (1:5000) and secondary polyclonal alkaline phosphatase (AP)-conjugated goat anti-rabbit immunoglobulin G (IgG) (1:10,000) (Sigma). GFP was detected using primary anti-GFP monoclonal serum (1:5000) (Zhongshan Jinqiao) and secondary polyclonal serum with AP-conjugated goat anti-mouse IgG (1:10,000) (Sigma)

Yeast two-Hybrid assay

Bait and prey plasmids were co-transformed into the yeast (Saccharomyces cerevisiae) strain AH109 and grown on double dropout medium (SD/–Leu/–Trp) at 30 °C for 5 days and then transferred to quadruple dropout medium (SD/–Ade/–His/–Leu/–Trp) supplemented with X-α-Gal.

Fluorescent protein imaging

GFP fluorescence on agroinfiltrated leaves was visualized using a UV handy lamp (Peking Liuyi model WD-9403E). Fluorescent protein expression in epidermal cells was observed using a Leica TCS SP5 CLSM.

Chemical and plasmolysis treatments

BFA (Sigma) and Lat B (Sigma) stocks were dissolved in DMSO and diluted with agroinfiltration buffer (Voinnet et al., 1998) to concentrations of $10\,\mu g\,ml^{-1}$ and $50\,\mu g\,ml^{-1}$, respectively, before infiltration of leaves. Four hours after infiltration, the leaves were observed by CLSM. For the control experiment, leaves were infiltrated with DMSO diluted in agroinfiltration buffer. For plasmolysis treatments, leaves were soaked in 10% (w/v) NaCl solution for 10 min and then observed by CLSM.

Hydrophobicity analysis and transmembrane prediction

Hydrophobicity plot generated with MPEx (http://blanco.biomol.uci.edu/mpex/) according to the Wimley and White octanol hydrophobicity scale (Wimley and White, 1996). For prediction of transmembrane domains, programs TopPred II (Claros and von Heijne, 1994; http://bioweb.pasteur.fr/seqanal/interfaces/toppred.html) and TMpred (Hofmann and Stoffel, 1993; http://www.ch.embnet.org/software/TMPRED_form.html) were used.

Acknowledgments

Appendix A. Supporting information

Supplementary data associated with this article can be found in the online version at http://dx.doi.org/10.1016/j.virol.2012.10.024.

References

An, H., Melcher, U., Doss, P., Payton, M., Guenzi, A.C., Verchot-Lubicz, J., 2003. Evidence that the 37 kDa protein of Soil-borne wheat mosaic virus is a virus movement protein. J. Gen. Virol. 84, 3153–3163.

Aridor, M., Weissman, J., Bannykh, S., Nuoffer, C., Balch, W.E., 1998. Cargo selection by the COPII budding machinery during export from the ER. J. Cell Biol. 141, 61–70.

Bamunusinghe, D., Hemenway, C.L., Nelson, R.S., Sanderfoot, A.A., Ye, C.M., Silva, M.A., Payton, M., Verchot-Lubicz, J., 2009. Analysis of potato virus X replicase and TGBp3 subcellular locations. Virology 393, 272–285.

Barlowe, C., 2003. Signals for COPII-dependent export from the ER: what's the ticket out? Trends Cell Biol. 13, 295–300.

Bayne, E., Rakitina, D., Morozov, S., Baulcombe, D., 2005. Cell-to-cell movement of potato potex virus X is dependent on suppression of RNA silencing. Plant J. 44, 471–482.

Benitez-Alfonso, Y., Faulkner, C., Ritzenthaler, C., Maule, A.J., 2010. Plasmodesmata: gateways to local and systemic virus infection. Mol. Plant Microbe Interact. 23, 1403–1412.

Boevink, P., Oparka, K.J., 2005. Virus-host interactions during movement processes. Plant Physiol. 138, 1815–1821.

Brill, L.M., Nunn, R.S., Kahn, T.W., Yeager, M., Beachy, R.N., 2000. Recombinant tobacco mosaic virus movement protein is an RNA-binding, alpha-helical membrane protein. Proc. Natl. Acad. Sci. USA 97, 7112–7117.

Cai, Y., Jia, T., Lam, S.K., Ding, Y., Gao, C., San, M.W., Pimpl, P., Jiang, L., 2011. Multiple cytosolic and transmembrane determinants are required for the trafficking of SCAMP1 via an ER-Golgi-TGN-PM pathway. Plant J. 65, 882–896.

Chen, M.H., Citovsky, V., 2003. Systemic movement of a tobamovirus requires host cell pectin methylesterase. Plant J. 35, 386–392.

Chen, M.H., Sheng, J., Hind, G., Handa, A.K., Citovsky, V., 2000. Interaction between the tobacco mosaic virus movement protein and host cell pectin methylesterases is required for viral cell-to-cell movement. EMBO J. 19, 913–920.

Chen, M.H., Tian, G.W., Gafni, Y., Citovsky, V., 2005. Effects of calreticulin on viral cell-to-cell movement. Plant Physiol. 138, 1866–1876.

Claros, M.G., von Heijne, G., 1994. TopPred II: an improved software for membrane protein structure predictions. CABIOS 10, 685–686.

Diao, A., Chen, J., Ye, R., Zheng, T., Yu, S., Antoniw, J., Adams, M., 1999. Complete sequence and genome properties of Chinese wheat mosaic virus, a new furovirus from China. J. Gen. Virol. 80, 1141–1145.

Genovés, A., Navarro, J.A., Pallás, V., 2010. The Intra- and inter-cellular movement of Melon necrotic spot virus (MNSV) depends on an active secretory pathway. Mol. Plant Microbe Interact. 23, 263–272.

Guenoune-Gelbart, D., Elbaum, M., Sagi, G., Levy, A., Epel, B.L., 2008. Tobacco mosaic virus (TMV) replicase and movement protein function synergistically in facilitating TMV spread by lateral diffusion in the plasmodesmal desmotubule of Nicotiana benthamiana. Mol. Plant Microbe Interact. 21, 335–345.

Harries, P.A., Schoelz, J.E., Nelson, R.S., 2010. Intracellular transport of viruses and their components: utilizing the cytoskeleton and membrane highways. Mol. Plant Microbe Interact. 23, 1381–1393.

Haupt, S., Cowan, G.H., Ziegler, A., Roberts, A.G., Oparka, K.J., Torrance, L., 2005. Two plant-viral movement proteins traffic in the endocytic recycling pathway. Plant Cell 17, 164–181.

Heinlein, M., 2002. The spread of tobacco mosaic virus infection: insights into the cellular mechanism of RNA transport. Cell. Mol. Life Sci. 59, 58–82.

Heinlein, M., Epel, B.L., Padgett, H.S., Beachy, R.N., 1995. Interaction of tobamovirus movement proteins with the plant cytoskeleton. Science 270, 1983–1985.

Heinlein, M., Padgett, H.S., Gens, J.S., Pickard, B.G., Casper, S.J., Epel, B.L., Beachy, R.N., 1998. Changing patterns of localization of the tobacco mosaic virus movement protein and replicase to the endoplasmic reticulum and microtubules during infection. Plant Cell 10, 1107–1120.

Herlitze, S., Koenen, M., 1990. A general and rapid mutagenesis method using polymerase chain reaction. Gene 91, 143–147.

Hofmann, K., Stoffel, W., 1993. TMbase—a database of membrane spanning proteins segments. Biol. Chem. Hoppe-Seyler 374, 166.

Hongo, S., Sato, K., Yokoyama, R., Nishitani, K., 2012. Demethylesterification of the primary wall by PECTIN METHYLESTERASE35 provides mechanical support to the arabidopsis stem. Plant Cell 24, 2624–2634.

Hu, C., Kerppola, T., 2003. Simultaneous visualization of multiple protein interactions in living cells using multicolor fluorescence complementation analysis. Nat. Biotechnol. 21, 539–545.

Huang, M., Zhang, L., 1999. Association of the movement protein of alfalfa mosaic virus with the endoplasmic reticulum and its trafficking in epidermal cells of onion bulb scale. Mol. Plant Microbe Interact. 12, 680–690.

Ju, H.J., Brown, J.E., Ye, C.M., Verchot-Lubicz, J., 2007. Mutations in the central domain of potato virus X TGBp2 eliminate granular vesicles and virus cell-to-cell trafficking. J. Virol. 81, 1899–1911.

Ju, H.J., Samuels, T.D., Wang, Y.S., Blancaflor, E., Payton, M., Mitra, R., Krishnamurthy, K., Nelson, R.S., Verchot-Lubicz, J., 2005. The potato virus X TGBp2 movement protein associates with endoplasmic reticulum-derived vesicles during virus infection. Plant Physiol. 138, 1877–1895.

Kaido, M., Tsuno, Y., Mise, K., Okuno, T., 2009. Endoplasmic reticulum targeting of the Red clover necrotic mosaic virus movement protein is associated with the replication of viral RNA1 but not that of RNA2. Virology 395, 232–242.

Kawakami, S., Watanabe, Y., Beachy, R.N., 2004. Tobacco mosaic virus infection spreads cell to cell as intact replication complexes. Proc. Natl. Acad. Sci. USA 101, 6291–6296.

Kost, B., Spielhofer, P., Chua, N.H., 1998. A GFP-mouse talin fusion protein labels plant actin filaments in vivo and visualizes the actin cytoskeleton in growing pollen tubes. Plant J. 16, 393–401.

Laporte, C., Vetter, G., Loudes, A.M., Robinson, D.G., Hillmer, S., Stussi-Garaud, C., Ritzenthaler, C., 2003. Involvement of the secretory pathway and the cytoskeleton in intracellular targeting and tubule assembly of Grapevine fanleaf virus movement protein in tobacco BY-2 cells. Plant Cell 15, 2058–2075.

Li, Y., Bao, Y.M., Wei, C.H., Kang, Z.S., Zhong, Y.W., Mao, P., Wu, G., Chen, Z.L., Schiemann, J., Nelson, R.S., 2004. Rice dwarf phytoreovirus segment S6-encoded nonstructural protein has a cell-to-cell movement function. J. Virol. 78, 5382–5389.

Lu, R., Malcuit, I., Moffett, P., Ruiz, M.T., Peart, J., Wu, A.J., Rathjen, J.P., Bendahmane, A., Day, L., Baulcombe, D.C., 2003. High throughput virus-induced gene silencing implicates heat shock protein 90 in plant disease resistance. EMBO J. 22, 5690–5699.

Martínez-Gil, L., Johnson, A.E., Mingarro, I., 2010. Membrane insertion and biogenesis of the Turnip crinkle virus p9 movement protein. J. Virol. 84, 5520–5527.

Martínez-Gil, L., Sánchez-Navarro, J.A., Cruz, A., Pallás, V., Pérez-Gil, J., Mingarro, I., 2009. Plant virus cell-to-cell movement is not dependent on the transmembrane disposition of its movement protein. J. Virol. 83, 5535–5543.

Maule, A.J., 2008. Plasmodesmata: structure, function and biogenesis. Curr. Opin. Plant Biol. 11, 680–686.

McLean, B.G., Zupan, J., Zambryski, P.C., 1995. Tobacco mosaic virus movement protein associates with the cytoskeleton in tobacco cells. Plant Cell 7, 2101–2114.

Melcher, U., 2000. The '30K' superfamily of viral movement proteins. J. Gen. Virol. 81, 257–266.

Miyashita, S., Kishino, H., 2010. Estimation of the size of genetic bottlenecks in cell-to-cell movement of soil-borne wheat mosaic virus and the possible role of the bottlenecks in speeding up selection of variations in trans-acting genes or elements. J. Virol. 84, 1828–1837.

Morozov, S.Y.u, Fedorkin, O.N., Jüttner, G., Schiemann, J., Baulcombe, D.C., Atabekov, J.G., 1997. Complementation of a potato virus X mutant mediated by bombardment of plant tissues with cloned viral movement protein genes. J. Gen. Virol. 78 (Pt 8), 2077–2083.

Nebenführ, A., Ritzenthaler, C., Robinson, D.G., 2002. Brefeldin A: deciphering an enigmatic inhibitor of secretion. Plant Physiol. 130, 1102–1108.

Nelson, B.K., Cai, X., Nebenführ, A., 2007. A multicolored set of in vivo organelle markers for co-localization studies in Arabidopsis and other plants. Plant J. 51, 1126–1136.

Ohno, T., Aoyagi, M., Yamanashi, Y., Saito, H., Ikawa, S., Meshi, T., Okada, Y., 1984. Nucleotide sequence of the tobacco mosaic virus (tomato strain) genome and comparison with the common strain genome. J. Biochem. 96, 1915–1923.

Peremyslov, V.V., Pan, Y.W., Dolja, V.V., 2004. Movement protein of a closterovirus is a type III integral transmembrane protein localized to the endoplasmic reticulum. J. Virol. 78, 3704–3709.

Pouwels, J., Van Der Krogt, G.N., Van Lent, J., Bisseling, T., Wellink, J., 2002. The cytoskeleton and the secretory pathway are not involved in targeting the cowpea mosaic virus movement protein to the cell periphery. Virology 297, 48–56.

Reichel, C., Beachy, R.N., 1998. Tobacco mosaic virus infection induces severe morphological changes of the endoplasmic reticulum. Proc. Natl. Acad. Sci. USA 95, 11169–11174.

Robinson, D.G., Herranz, M.-C., Bubeck, J., Pepperkok, R., Ritzenthaler, C., 2007. Membrane dynamics in the early secretory pathway. Crit. Rev. Plant Sci. 26, 199–225.

Schoelz, J.E., Harries, P.A., Nelson, R.S., 2011. Intracellular transport of plant viruses: finding the door out of the cell. Mol. Plant 4, 813–831.

Shimizu, T., Yoshii, A., Sakurai, K., Hamada, K., Yamaji, Y., Suzuki, M., Namba, S., Hibi, T., 2009. Identification of a novel tobacco DnaJ-like protein that interacts with the movement protein of tobacco mosaic virus. Arch. Virol. 154, 959–967.

Sun, L., Suzuki, N., 2008. Intragenic rearrangements of a mycoreovirus induced by the multifunctional protein p29 encoded by the prototypic hypovirus CHV1-EP713. RNA 14, 2557–2571.

Tagami, Y., Watanabe, Y., 2007. Effects of brefeldin A on the localization of Tobamovirus movement protein and cell-to-cell movement of the virus. Virology 361, 133–140.

Tilsner, J., Cowan, G.H., Roberts, A.G., Chapman, S.N., Ziegler, A., Savenkov, E., Torrance, L., 2010. Plasmodesmal targeting and intercellular movement of potato mop-top pomovirus is mediated by a membrane anchored tyrosine-based motif on the lumenal side of the endoplasmic reticulum and the C-terminal transmembrane domain in the TGB3 movement protein. Virology 402, 41–51.

Tomenius, K., Clapham, D., Meshi, T., 1987. Localization by immunogold cytochemistry of the virus-coded 30K protein in plasmodesmata of leaves infected with tobacco mosaic virus. Virology 160, 363–371.

Ueki, S., Spektor, R., Natale, D.M., Citovsky, V., 2010. ANK, a host cytoplasmic receptor for the Tobacco mosaic virus cell-to-cell movement protein, facilitates intercellular transport through plasmodesmata. PLoS Pathog. 6, e1001201.

Verchot-Lubicz, J., Torrance, L., Solovyev, A.G., Morozov, S.Y., Jackson, A.O., Gilmer, D., 2010. Varied movement strategies employed by triple gene block-encoding viruses. Mol. Plant Microbe Interact. 23, 1231–1247.

Vogel, F., Hofius, D., Sonnewald, U., 2007. Intracellular trafficking of Potato leafroll virus movement protein in transgenic Arabidopsis. Traffic 8, 1205–1214.

Voinnet, O., Lederer, C., Baulcombe, D.C., 2000. A viral movement protein prevents spread of the gene silencing signal in Nicotiana benthamiana. Cell 103, 157–167.

Voinnet, O., Rivas, S., Mestre, P., Baulcombe, D., 2003. An enhanced transient expression system in plants based on suppression of gene silencing by the p19 protein of tomato bushy stunt virus. Plant J. 33, 949–956.

Voinnet, O., Vain, P., Angell, S., Baulcombe, D.C., 1998. Systemic spread of sequence-specific transgene RNA degradation in plants is initiated by localized introduction of ectopic promoterless DNA. Cell 95, 177–187.

Wei, T., Wang, A., 2008. Biogenesis of cytoplasmic membranous vesicles for plant potyvirus replication occurs at endoplasmic reticulum exit sites in a COPI- and COPII-dependent manner. J. Virol. 82, 12252–12264.

Wimley, W.C., White, S.H., 1996. Experimentally determined hydrophobicity scale for proteins at membrane interfaces. Nat. Struct. Biol. 3, 842–848.

Wright, K.M., Wood, N.T., Roberts, A.G., Chapman, S., Boevink, P., Mackenzie, K.M., Oparka, K.J., 2007. Targeting of TMV movement protein to plasmodesmata requires the actin/ER network: evidence from FRAP. Traffic 8, 21–31.

Xiong, R., Wu, J., Zhou, Y., Zhou, X., 2008. Identification of a movement protein of the tenuivirus rice stripe virus. J. Virol. 82, 12304–12311.

Yang, J., Chen, J., Chen, J., Jiang, H., Zhao, Q., Adams, M.J., 2001. Sequence of a second isolate of Chinese wheat mosaic furovirus. J. Phytopathol. 149, 135–140.

Zhang, C., Machray, G.C., Cruz, S.S., Wilson, T.M.A., 2005. Soil-borne wheat mosaic virus (SBWMV) 37 kDa protein rescues cell-to-cell and long-distance movement of an immobile tobacco mosaic virus mutant in Nicotiana benthamiana, a non-host of SBWMV. J. Phytopathol. 153, 5–10.